

CrossMark  
click for updatesCite this: *Anal. Methods*, 2015, 7, 1328

# A novel photoelectrochemical sensor for the detection of $\alpha$ -fetoprotein based on a mesoporous TiO<sub>2</sub>–CdS QD composite film†

Xiaoyan Yang,\* Jingyu Li and Junliang Fu

In this article, a label-free photoelectrochemical immunosensor based on a CdS-modified mesoporous TiO<sub>2</sub> film has been developed. The CdS quantum dots could be deposited onto the mesoporous TiO<sub>2</sub> film by electrochemical deposition, which could enhance the photocurrent intensity in the visible region. Employing specific binding of antigen–antibody,  $\alpha$ -fetoprotein (AFP) could be captured on the surface of the modified electrode. Based on the steric hindrances, the photocurrent intensity decreased with the increase in AFP concentration. A linear response from 0.05 ng mL<sup>-1</sup> to 20 ng mL<sup>-1</sup> was obtained for AFP detection and the detection limit was 0.02 ng mL<sup>-1</sup>. Moreover, the practical determination of AFP in human serum was also investigated.

Received 16th October 2014  
Accepted 11th December 2014

DOI: 10.1039/c4ay02473g

www.rsc.org/methods

## 1 Introduction

Proteins are ubiquitous in all living organisms and play an essential role in biochemical systems. In particular, many disease-marker proteins that are used to diagnose the early stage of disease or pathological conditions are often present at a very low concentration. Accordingly, the specific identification and sensitive detection of proteins are of tremendous importance in fundamental research and clinical diagnostic.

During recent years, the photoelectrochemical (PEC) analysis has become a new topic and technology for biological detection due to its remarkable sensitivity, simple instrumentation, easy integration and low-cost.<sup>1–4</sup> In the PEC technique, upon photoirradiation, the electron could transfer among the analyte, semiconductor and electrode, and the change of photocurrent intensity could be recorded.<sup>5</sup> Owing to the complete separation of the excitation source (light) and detection signal (photocurrent), the photoelectrochemical method has low background and high sensitivity in many potential applications.<sup>2,6</sup> Some metal oxide semiconductors have been used widely as photoelectrochemical materials, such as ZnO, ZrO<sub>2</sub> and TiO<sub>2</sub>.<sup>7</sup>

As a typical n-type semiconductor, TiO<sub>2</sub> owns extensive applications because of its wide band gap, good biocompatibility and high photoelectrochemical activity under UV light irradiation.<sup>8</sup> A variety of states of TiO<sub>2</sub> including TiO<sub>2</sub> nanorods and mesoporous TiO<sub>2</sub> have been tested in photoelectrochemical

experiments and satisfactory results have been obtained.<sup>9–11</sup> With high pore volume, the mesoporous TiO<sub>2</sub> has a large specific surface area and strong surface adsorption ability. Antibodies and other biomolecules could be easily combined on the TiO<sub>2</sub> surface and pore channels through electrostatic adsorption.<sup>12</sup> Compared with chemical binding between biomolecules and electrodes, electrostatic adsorption on the mesoporous TiO<sub>2</sub> surface could make the operation simpler. However, the wide band gap (~3.2 eV) impedes the application of the TiO<sub>2</sub> semiconductor.<sup>8</sup> In particular, the UV light could damage the biological activity of many biomolecules such as DNA, antigens, antibodies, *etc.*<sup>13,14</sup> Therefore, it was difficult to achieve the photoelectrochemical immunoassay using TiO<sub>2</sub> which could only absorb the UV light. To address this drawback, different amplification strategies were developed,<sup>15,16</sup> such as sensitization with dyes, doping with other impurities and coupling with narrow band gap semiconductors. As a significant semiconductor material, quantum dots (QDs) have been widely used for photoelectrochemical detection due to their unique characteristics such as favourable size, broad excitation spectra and active surface properties.<sup>17–20</sup> By combining TiO<sub>2</sub> and QDs together, the two semiconductor materials could provide stability in photocatalytic activities.<sup>21</sup>

Herein, a label-free PEC immunosensor based on a CdS-modified mesoporous TiO<sub>2</sub> film is presented for protein detection. AFP, an important protein for the diagnosis of hepatocellular carcinoma (HCC),<sup>22</sup> was selected as the model protein. In this work, the CdS QDs could be achieved in one-step on the surface and channel of the mesoporous TiO<sub>2</sub> thin film by electrochemical deposition. The photocurrent intensity could be enhanced dramatically by the TiO<sub>2</sub> film modified with CdS QDs. After that, the illumination light has been changed to the visible range.<sup>23</sup> The AFP antibody could be combined on the

Shandong Provincial Key Laboratory of Biochemical Analysis, College of Chemistry and Molecular Engineering, Qingdao University of Science and Technology, Qingdao 266042, Shandong, P. R. China. E-mail: yangxiaoyan\_zh@126.com; Fax: +86-532-84022700; Tel: +86-532-84022700

† Electronic supplementary information (ESI) available. See DOI: 10.1039/c4ay02473g

CdS/TiO<sub>2</sub> electrode through an immunoreaction. AFP could be quantified in the range of 0.05 ng mL<sup>-1</sup> to 20 ng mL<sup>-1</sup> with the detection limit of 0.02 ng mL<sup>-1</sup>. Moreover, due to the high affinity and specificity of immunoassay, the label-free biosensing system exhibited not only high sensitivity and specificity but also excellent performance in real human serum assay.

## 2 Experimental

### 2.1 Reagents

Tetrabutyl titanate (TBOT, 5593-70-4), ascorbic acid (50-81-7), cadmium chloride (CdCl<sub>2</sub>, 10108-64-2), and sodium thiosulfate pentahydrate (Na<sub>2</sub>S<sub>2</sub>O<sub>3</sub>·5H<sub>2</sub>O, 10102-17-7) were purchased from Aladdin CHEMICAL (Shanghai, China); P123 (9003-11-6) was purchased from J&K CHEMICAL (Beijing, China); and AFP antigen and AFP antibody were purchased from Biosynthesis Biotechnology Co., Ltd (Beijing, China). Analytical reagent grade chemicals and deionized, doubly distilled water were used throughout.

### 2.2 Apparatus

Photoelectrochemical measurements were carried out with a MPI-EO analyzer (XiAn Remex Analysis Instrument Co. Ltd). The Atomic Force Microscopy (AFM) image was taken with a Being Nano-Instruments CSPM-4000 (Benyuan, China). X-Ray measurements were performed on a D/max2500 PC diffractometer (RIGAKU) using Cu-K $\alpha$  radiation. The scanning electron microscopy (SEM) image was taken with a JSM-6700F instrument (HITACHI). The TiO<sub>2</sub>/ITO film was prepared with a spin coater (Siyouen Electronics Technology Co. Ltd., Beijing, China). A three-electrode system was employed with Pt wire as an auxiliary electrode, Ag/AgCl as a reference electrode and indium tin oxide (ITO) glass as a working electrode. Prior to use, the ITO-coated glass was cleaned in an ultrasonic cleaner with each of the following solutions sequentially: deionized water (2 min, twice), ethanol (20 min), acetone (20 min) and deionized water (10 min, twice).

### 2.3 Synthesis of the mesoporous TiO<sub>2</sub> thin film

The TiO<sub>2</sub> sol was prepared by the hydrolysis method described previously with a slight modification.<sup>23</sup> HCl solution (5 mL, 37%) was added to ethanol water solution (40 mL) under vigorous stirring. Ti(OC<sub>4</sub>H<sub>9</sub>)<sub>4</sub> (5 mL) was dissolved in ethanol (20 mL) at room temperature under vigorous stirring for 3 h. The Ti(OC<sub>4</sub>H<sub>9</sub>)<sub>4</sub> solution was added to HCl mixture solution at room temperature under vigorous stirring for 1.5 h. P123 (1.8 g) used as the template was dissolved in ethanol (25 mL), and then added to the Ti(OC<sub>4</sub>H<sub>9</sub>)<sub>4</sub> solution. The solution was aged with stirring at room temperature for 30 min to obtain TiO<sub>2</sub> sol. ITO-coated glass was cleaned in an ultrasonic cleaner. The TiO<sub>2</sub> sol was coated with a spin coater operating at 300 rpm for 3 s, and then the speed of the spin coater was increased to 2000 rpm for 10 s. The film was aged at room temperature for 24 h, and then calcined at 480 °C for 2 h in order to remove the template. The TiO<sub>2</sub> mesoporous film was then deposited onto 8 × 50 mm<sup>2</sup> sized slides of ITO.

### 2.4 Preparation of the CdS-mesoporous TiO<sub>2</sub> composite film

The electrochemical deposition process was achieved with Pt wire as an auxiliary electrode, Ag/AgCl as a reference electrode and TiO<sub>2</sub>/ITO as a working electrode in an electrolyte containing CdCl<sub>2</sub> (0.1 M) and Na<sub>2</sub>S<sub>2</sub>O<sub>3</sub>·5H<sub>2</sub>O (0.01 M) at pH = 2 and temperature at 40 °C. The deposition potential was -0.7 V and deposition time was 25 min.

### 2.5 Construction of the immunosensor

By dissolving chitosan (CS) powder in acetic acid (1%) the CS solution (0.5 wt%) was obtained. The CS solution (30  $\mu$ L) was dropped onto the CdS/TiO<sub>2</sub>/ITO electrode and dried at room temperature and the CdS/TiO<sub>2</sub>/ITO electrode was washed with NaOH solution (0.1 M) and distilled water. Glutaraldehyde (GLD) (30  $\mu$ L) was dropped onto the CS/CdS/TiO<sub>2</sub>/ITO electrode and aged at room temperature for 30 min. The electrode was washed with distilled water. The AFP antibody (30  $\mu$ L, 50  $\mu$ g mL<sup>-1</sup>) was dropped onto the CS/CdS/TiO<sub>2</sub>/ITO electrode and aged at 4 °C for 12 h. The electrode was washed with phosphate buffer solution (NaH<sub>2</sub>PO<sub>4</sub>-Na<sub>2</sub>HPO<sub>4</sub>, PBS, 0.01 M, pH = 7.4). Finally, the electrode was incubated with Bovine Serum Albumin (BSA) for 30 min at 37 °C to block nonspecific binding sites. After washing with PBS buffer solution, the electrode was incubated in different concentrations of AFP for 1 h at 37 °C, and then was used for PEC detection.

### 2.6 Analysis of AFP

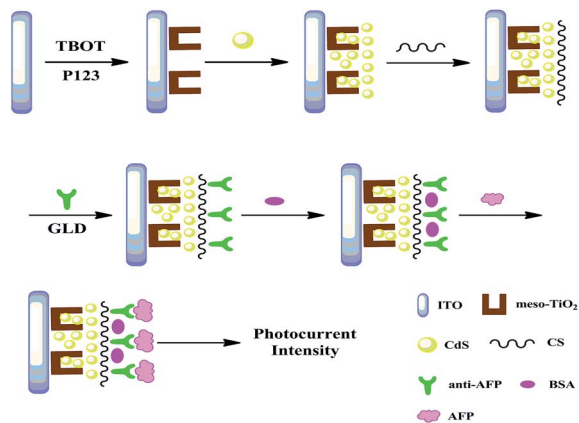
The photoelectrochemical detection was achieved with Pt wire as an auxiliary electrode, Ag/AgCl as a reference electrode and anti-AFP/CdS/TiO<sub>2</sub>/ITO as a working electrode in PBS buffer solution (0.01 M, pH = 7.4) containing ascorbic acid solution (0.1 M) as the electron donor which could stabilize the photocurrent signal with the illumination light at 400 nm.

## 3 Results and discussion

### 3.1 Characterization of the development of the immunosensor

The preparation process of the immunosensor and the detection strategy are shown in Scheme 1. The mesoporous TiO<sub>2</sub> thin film was first obtained on the surface of the ITO electrode by the calcination procedure. CdS QDs were deposited on the TiO<sub>2</sub>/ITO electrode through the electrochemical deposition process. As a result, the illumination light of the TiO<sub>2</sub>/ITO electrode was changed to the visible range, and the photocurrent intensity was enhanced dramatically. The anti-AFP was anchored on the surface of the CS/CdS/TiO<sub>2</sub>/ITO by covalent conjugation. After blocking with BSA, the assembled ITO electrode was introduced to the immunoreaction with the exposed part of AFP by an incubation period. With the increase of the concentration of AFP, the photocurrent intensity would be decreased.

Fig. 1 shows the surface topography of the ITO electrode modified with different materials through the AFM images. Fig. 1A presents the image of mesoporous TiO<sub>2</sub>/ITO. Fig. 1B shows the image of the TiO<sub>2</sub>/ITO electrode modified with CdS QDs. The coverage of CdS QDs generated a different topography



Scheme 1 Schematic diagram of the PEC immunosensor fabrication process.

compared with the  $\text{TiO}_2/\text{ITO}$  electrode, and the film became thicker than that of the  $\text{TiO}_2/\text{ITO}$  electrode clearly. The SEM results (Fig. S1†) also indicated that the CdS QDs were successfully deposited onto the surface of the  $\text{TiO}_2/\text{ITO}$  electrode. Fig. 1C shows the surface topography after the covalent immobilization of anti-AFP on the CdS/ $\text{TiO}_2$  composite film. After combining with anti-AFP, the thickness and surface topography in AFM images changed. It indicated that the anti-AFP was immobilized on the CdS/ $\text{TiO}_2/\text{ITO}$  electrode successfully. When the AFP antigen was captured on the electrode, the surface intensity of the electrode increased. The AFM image of the electrode surface combined with AFP antigen is shown in Fig. 1D. After comparison between part C and part D, it is shown that the surface topography of part D is more compact and different.

As shown in Fig. 2A, the low-angle diffraction peak at  $2\theta = 1.0$  confirmed the presence of a mesoporous structure in the  $\text{TiO}_2$  film on the ITO glass.<sup>24</sup> After modifying with CdS QDs on the  $\text{TiO}_2$  film, the low-angle diffraction peak at  $2\theta = 1.0$  was lost (as shown in Fig. 2C), which might be caused by pore filling with CdS QDs. The characteristic peaks of (101), (004), (200), (105) were attributed to diffraction peaks of anatase  $\text{TiO}_2$  (as shown in Fig. 2B and D).<sup>25,26</sup>

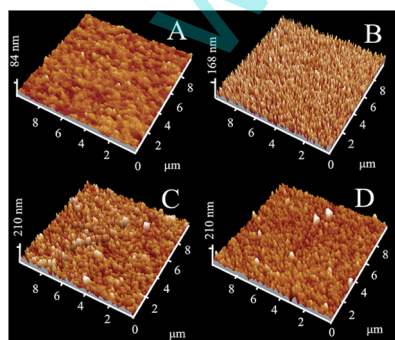


Fig. 1 AFM topography images of (A) mesoporous  $\text{TiO}_2/\text{ITO}$ ; (B) CdS/ $\text{TiO}_2/\text{ITO}$ ; (C) anti-AFP/CdS/ $\text{TiO}_2/\text{ITO}$ ; and (D) AFP/anti-AFP/CdS/ $\text{TiO}_2/\text{ITO}$ .

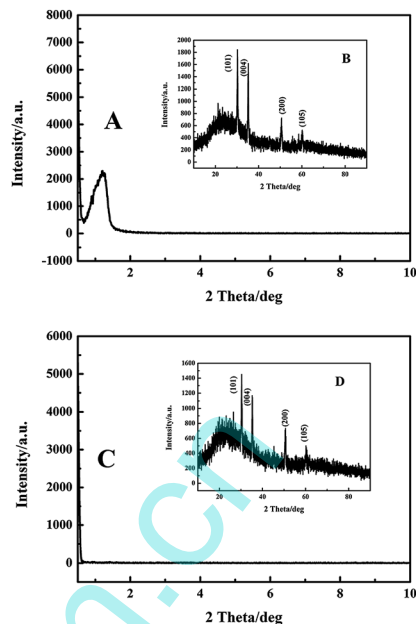


Fig. 2 (A) Low-angle X-ray diffraction pattern and (B) wide-angle X-ray diffraction pattern of the  $\text{TiO}_2$  film on the ITO glass. (C) Low-angle X-ray diffraction pattern and (D) wide-angle X-ray diffraction pattern of the CdS/ $\text{TiO}_2/\text{ITO}$  film.

The  $\text{TiO}_2$  semiconductor could only absorb the UV light, which limited its application. CdS was a low band gap semiconductor material. However, coupling of  $\text{TiO}_2$  with CdS QDs could make  $\text{TiO}_2$  absorb visible light and greatly improve the photocurrent efficiency. The mesoporous  $\text{TiO}_2$  thin films on the ITO electrode were modified with the CdS QDs by electrochemical deposition. The photocurrent intensity comparison between the  $\text{TiO}_2/\text{ITO}$  electrode (b) and CdS/ $\text{TiO}_2/\text{ITO}$  electrode (a) in 0.01 M PBS buffer solution (pH = 7.4) containing 0.1 M ascorbic acid solution as the electron donor with a light excitation at 400 nm is shown in Fig. S2 (ESI†). The photocurrent intensity was enhanced clearly indicating that the CdS QDs had been successfully deposited on the  $\text{TiO}_2/\text{ITO}$  electrode. The wavelength scanning is shown in Fig. S3 and S4 (ESI†). It could be seen that CdS QDs expanded the absorption of the  $\text{TiO}_2$  film from the UV region to visible region.

### 3.2 Feasibility of the assay

As an effective method to characterize surface modifications and assembling processes on the electrode, the electrochemical impedance spectra (EIS) of the development of the immunosensor are shown in Fig. 3A. The CdS/ $\text{TiO}_2/\text{ITO}$  electrode (a) showed a small semicircle. After immobilizing chitosan (CS) on the CdS/ $\text{TiO}_2/\text{ITO}$  electrode, the impedance spectrum (b) was increased. When the anti-AFP (c) was covalently combined with the CdS/ $\text{TiO}_2/\text{ITO}$  electrode, the resistance  $R_{\text{et}}$  increased. After blocking with BSA (d) and the specific immunoreaction between anti-AFP and AFP (e), the  $R_{\text{et}}$  still increased gradually. The reason for the increase of the resistance  $R_{\text{et}}$  was that the layer on the electrode increased in the experimental process. The

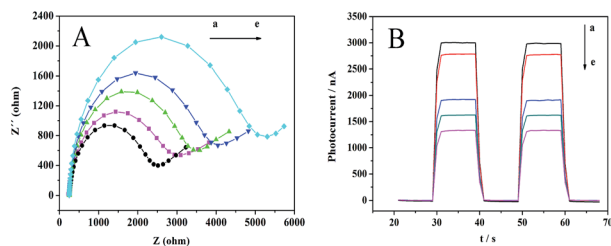


Fig. 3 EIS of the immunosensor and photocurrent responses of the immunosensor.

electron transfer between the electrode and the electrolyte solution was obstructed.

As shown in Fig. 3B, the change of photocurrent intensity was recorded for characterising the fabrication process of the photoelectrochemical immunoassay sensor. The current intensity of the CdS/TiO<sub>2</sub>/ITO (a) electrode was about 3000 nA. The current intensity was reduced after immobilizing with anti-AFP (c) through covalently combining with the –NH<sub>2</sub> of chitosan (CS) (b) and blocking with BSA (d). After that, the photocurrent intensity was reduced clearly because of the specific recognition to AFP (e). The photocurrent intensity has been reduced after immobilizing with the biomolecule, because the biomolecule could increase the steric hindrances on the surface of the electrode. Thus, it indicated that the biomolecule had been successfully immobilized on the composite electrode. At the same time, the change of photocurrent intensity could be used for the quantitative analysis of the biomolecule in clinical practice.

### 3.3 Condition optimization of the immunosensor

The optimization of the deposition time is shown in Fig. S5 (ESI†). The effect of the deposition time on the photocurrent responses was examined in the range of 5 to 35 min. It was found that the photocurrent intensity was enhanced along with the increase of deposition time. However, with the increase of time, the photocurrent intensity became lower, because the

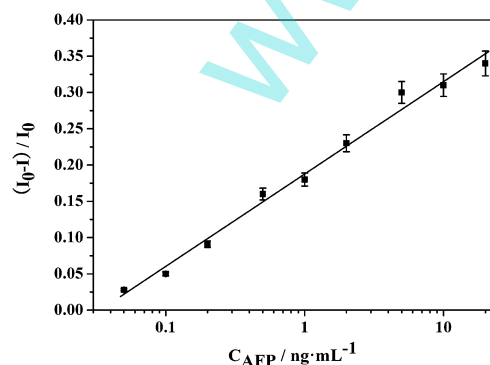


Fig. 4 Calibration curve corresponding to the analysis of different concentrations of AFP from 0.05 ng mL<sup>-1</sup> to 20 ng mL<sup>-1</sup>.  $I_0$  and  $I$  were the photocurrent intensities of BSA/anti-AFP/CS/CdS/TiO<sub>2</sub>/ITO and AFP/BSA/anti-AFP/CS/CdS/TiO<sub>2</sub>/ITO.

films on the ITO electrode became thicker than before. It indicated that the optimized deposition time is 25 min.

The optimization of the concentration of anti-AFP is shown in Fig. S6 (ESI†). In order to study the influence of the amount of the anti-AFP immobilized on the surface of the ITO electrode, different concentrations of anti-AFP were added.  $I_0$  and  $I$  were the photocurrent intensities of CS/CdS/TiO<sub>2</sub>/ITO and anti-AFP/CS/CdS/TiO<sub>2</sub>/ITO. With the increase of the concentration of anti-AFP, the  $(I_0 - I)/I_0$  was reduced. When the concentration of anti-AFP exceeded 50 μg mL<sup>-1</sup>, the  $(I_0 - I)/I_0$  kept unchanged. Therefore, the optimized concentration of anti-AFP was 50 μg mL<sup>-1</sup>.

### 3.4 Analytical performance of the immunosensor

After incubating with different concentrations of AFP, the process of quantifying the behavior of the immunosensor has been achieved. Fig. 4 shows a linear relationship between the photocurrent intensity and the concentration of AFP. The regression equation was  $(I_0 - I)/I_0 = 0.1876 + 0.1273 \log C$  (ng mL<sup>-1</sup>), where  $I_0$  and  $I$  were the photocurrent intensities of BSA/anti-AFP/CS/CdS/TiO<sub>2</sub>/ITO and AFP/BSA/anti-AFP/CS/CdS/TiO<sub>2</sub>/ITO, with a regression coefficient of 0.9947. The immunoassay showed a linear range for AFP from 0.05 ng mL<sup>-1</sup> to 20 ng mL<sup>-1</sup> with the detection limit of 0.02 ng mL<sup>-1</sup>.

### 3.5 Selectivity of the AFP assay

Control experiments were performed by recording the photocurrent intensity of carcinoembryonic antigen (CEA) (10 ng mL<sup>-1</sup>), Tn antigen (10 ng mL<sup>-1</sup>), AFP (1.0 ng mL<sup>-1</sup>) and the mixed sample including CEA (10 ng mL<sup>-1</sup>), Tn antigen (10 ng mL<sup>-1</sup>) and AFP (1.0 ng mL<sup>-1</sup>) as shown in Fig. 5. The photocurrent intensity has been changed by adding AFP because of the recognition effect between anti-AFP and AFP. The  $(I_0 - I)/I_0$  value of CEA and Tn antigen was much lower than that of AFP. Moreover, the photocurrent intensity of the AFP and the mixed sample was almost the same because of the specific immunobinding. It indicated a good selectivity for this immunoassay sensor.

### 3.6 Practical determination of AFP in human serum

To demonstrate the feasibility of the immunoassay system for the practical clinical analysis, standard addition was performed by adding a standard concentration of AFP to human serum

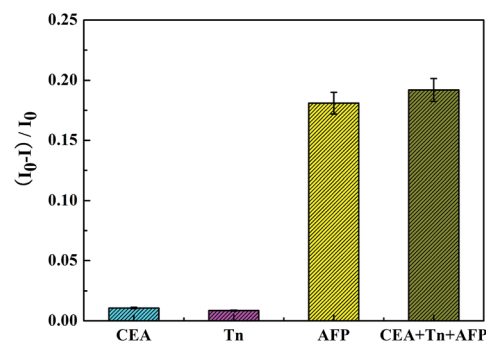


Fig. 5 Selectivity toward different analytes (CEA, Tn, AFP).



samples. As shown in Table S1 (ESI<sup>†</sup>), the recoveries ranged from 94.6% to 109%, and the average recoveries were 103%. The relative deviation was 3.5%. All the results indicated the reliability of this assay. Therefore, this method could be used to monitor the content of ATP in human serum without the interference of other substances.

## 4 Conclusions

In this work, a label-free photoelectrochemical immunosensor has been established. Because of the large specific surface area of mesoporous TiO<sub>2</sub>, the adsorption capacity was enhanced. It is easier to modify CdS QDs on the mesoporous TiO<sub>2</sub> film. The photocurrent intensity has been enhanced and the illumination light could be changed to the visible range by electrochemical deposition of the CdS QDs on the mesoporous TiO<sub>2</sub> film. In this analytical process, a direct quantitative analysis of AFP has been achieved without other label molecules, and good sensitivity and selectivity were obtained. Therefore, the proposed immunosensor exhibited ease of operation, low-cost, high efficiency and excellent sensitivity. More importantly, the results in real human serum assay implied that the strategy could be a useful analytical tool in biological research and clinical diagnostics.

## Acknowledgements

This research was supported by the National Nature Science Foundation of China (no. 21005044), the Excellent Young Scientists Encouragement Foundation of Shandong Province (BS2011CL017), and the Program for Changjiang Scholars and Innovative Research Team in University (PCSIRT).

## Notes and references

- 1 K. Wang, J. Wu, Q. Liu, Y. C. Jin, J. J. Yan and J. R. Cai, *Anal. Chim. Acta*, 2012, **745**, 131.
- 2 H. Y. Wu, J. C. Hu, H. Li and H. X. Li, *Sens. Actuators, B*, 2013, **182**, 802.
- 3 W. Zhao, J. Xu and H. Chen, *Chem. Soc. Rev.*, 2015, DOI: 10.1039/c4cs00228h.
- 4 W. Zhao, J. Xu and H. Chen, *Chem. Rev.*, 2014, **114**, 7421.
- 5 Y. Q. Hu, Z. H. Xue, H. X. He, R. X. Ai and X. H. Liu, *Biosens. Bioelectron.*, 2013, **47**, 45.
- 6 S. P. Jia, M. M. Liang and L. H. Guo, *J. Phys. Chem. B*, 2008, **112**, 4461.
- 7 W. W. Tu, Y. T. Dong, J. P. Lei and H. X. Ju, *Anal. Chem.*, 2010, **82**, 8711.
- 8 H. B. Li, J. Li, Q. Xu and X. Y. Hu, *Anal. Chem.*, 2011, **83**, 9681.
- 9 D. S. Kim and S. Y. Kwak, *Environ. Sci. Technol.*, 2009, **43**, 148.
- 10 Y. Zhang, A. H. Yuwono, J. Wang and J. Li, *J. Phys. Chem. C*, 2009, **113**, 21406.
- 11 R. Fateh, A. A. Ismail, R. Dillert and D. W. Bahnemann, *J. Phys. Chem. C*, 2011, **115**, 10405.
- 12 G. Cheng, Z. G. Wang, Y. L. Liu, J. L. Zhang, D. H. Sun and J. Z. Ni, *ACS Appl. Mater. Interfaces*, 2013, **5**, 3182.
- 13 G. L. Wang, J. J. Xu and H. Y. Chen, *Biosens. Bioelectron.*, 2009, **24**, 2494.
- 14 J. S. Katz, J. S. Doh and D. J. Irvine, *Langmuir*, 2006, **22**, 353.
- 15 Y. L. Lee, C. F. Chi and S. Y. Liau, *Chem. Mater.*, 2009, **22**, 922.
- 16 M. M. Liang, S. L. Liu, M. Y. Wei and L. H. Guo, *Anal. Chem.*, 2006, **78**, 621.
- 17 W. W. Zhao, Z. Y. Ma, P. P. Yu, X. Y. Dong, J. J. Xu and H. Y. Chen, *Anal. Chem.*, 2012, **84**, 917.
- 18 W. W. Zhao, J. Wang, J. J. Xu and H. Y. Chen, *Chem. Commun.*, 2011, **47**, 10990.
- 19 X. Y. Li, C. G. Hu, Z. H. Zhao, K. Y. Zhang and H. Liu, *Sens. Actuators, B*, 2013, **182**, 461.
- 20 P. K. Santra and P. V. Kamat, *J. Am. Chem. Soc.*, 2013, **135**, 877.
- 21 W. T. Sun, Y. Yu, H. Y. Pan, X. F. Gao, Q. Chen and L. M. Peng, *J. Am. Chem. Soc.*, 2008, **130**, 1124.
- 22 W. B. Liang, R. Yuan, Y. Q. Chai, Y. Li and Y. Zhuo, *Electrochim. Acta*, 2008, **53**, 2302.
- 23 Q. Kang, L. X. Yang, Y. F. Chen, S. L. Luo, L. F. Wen, Q. Y. Cai and S. Z. Yao, *Anal. Chem.*, 2010, **82**, 9749.
- 24 G. F. Fu, P. S. Vary and C. T. Lin, *J. Phys. Chem. B*, 2005, **109**, 8889.
- 25 J. C. Tao, Y. Sun, M. Y. Ge, X. Chen and N. Dai, *ACS Appl. Mater. Interfaces*, 2010, **2**, 265.
- 26 L. P. Liu, J. Hensel, R. C. Fitzmorris, Y. D. Li and J. Z. Zhang, *J. Phys. Chem. Lett.*, 2010, **1**, 155.